Comparison of radiological and clinical features of temporal lobe necrosis in nasopharyngeal carcinoma patients treated with 2D radiotherapy or intensity-modulated radiotherapy

Y-P Mao[1,7], G-Q Zhou[1,7], L-Z Liu[2], R Guo[1], Y Sun[1], L Li[2], A-H Lin[3], M-S Zeng[4], T-B Kang[4], W-H Jia[4], J-Y Shao[5], H-Q Mai[6] and J Ma*,[1]

[1]State Key Laboratory of Oncology in Southern China, Collaborative Innovation Center of Cancer Medicine, Department of Radiation Oncology, Cancer Center, Sun Yat-sen University, 651 Dongfeng Road East, Guangzhou 510060, People's Republic of China; [2]State Key Laboratory of Oncology in Southern China, Collaborative Innovation Center of Cancer Medicine, Imaging Diagnosis and Interventional Center, Cancer Center, Sun Yat-sen University, Guangzhou 510060, People's Republic of China; [3]Department of Medical Statistics and Epidemiology, School of Public Health, Sun Yat-sen University, Guangzhou 510060, People's Republic of China; [4]State Key Laboratory of Oncology in Southern China, Collaborative Innovation Center of Cancer Medicine, Cancer Center, Sun Yat-sen University, Guangzhou 510060, People's Republic of China; [5]State Key Laboratory of Oncology in Southern China, Collaborative Innovation Center of Cancer Medicine, Department of Molecular Diagnostics, Cancer Center, Sun Yat-sen University, Guangzhou 510060, People's Republic of China and [6]State Key Laboratory of Oncology in Southern China, Collaborative Innovation Center of Cancer Medicine, Department of Nasopharyngeal Cancer, Cancer Center, Sun Yat-sen University, Guangzhou 510060, People's Republic of China

Background: To compare the imaging and clinical features of temporal lobe necrosis (TLN) in nasopharyngeal carcinoma (NPC) patients treated with two-dimensional radiotherapy (2D-RT) or those with intensity-modulated radiotherapy (IMRT).

Methods: We retrospectively analysed NPC patients who underwent 2D-RT (72 patients, 128 temporal lobes) or IMRT (36 patients, 50 lobes) and developed radiation-induced, MRI-confirmed TLN.

Results: White-matter lesions (WMLs), contrast-enhanced lesions, cysts and local mass effects were present in 128 out of 128 vs 48 out of 50 ($P = 0.078$), 123 out of 128 vs 47 out of 50 ($P = 0.688$), 10 out of 128 vs 1 out of 50 ($P = 0.185$) and 57 out of 128 vs 13 out of 50 ($P = 0.023$) temporal lobes, respectively, in the 2D-RT and IMRT groups. The WMLs were more extensive in the 2D-RT group ($P < 0.001$). The maximum diameter of contrast-enhanced lesions was greater in the 2D-RT group ($P < 0.001$), and these lesions tended to extend far away from the nasopharynx. The WMLs and enhancement had no impact on cyst development (both $P = 1$). Local mass effects were always accompanied with contrast-enhanced lesions ($P = 0.024$) but were not correlated with WMLs or cysts ($P = 0.523$ and 0.341, respectively). There were no between-group differences in clinical features (all P-values > 0.05), whereas the difference in the incidence of severe debility was of marginal significance (18.1% vs 5.6%, $P = 0.077$).

Conclusions: The IMRT-induced TLN was less extensive and milder than 2D-RT-induced TLN, but both had similar clinical features.

Nasopharyngeal carcinoma (NPC) is a very common malignancy in the southern Chinese population (Jemal *et al*, 2011). Radical radiotherapy (RT) remains the primary treatment modality for non-disseminated NPC because of its anatomic location and radiosensitivity. For decades, two-dimensional radiotherapy (2D-RT) was used via laterally opposed fields. Overall, disease control using 2D-RT has been satisfactory. However, 2D-RT inevitably exposed parts of the temporal lobes close to the nasopharynx to high doses of radiation (Lee *et al*, 1990, 1992).

In the management of NPC, incidental irradiation of the temporal lobe with consequent long-term injury is one of the most feared complications after radical RT, as it can be devastating for patients and is associated with severe impairment of quality of life (Lee *et al*, 1992). Temporal lobe necrosis (TLN) was usually diagnosed via brain computed tomography or magnetic resonance imaging (MRI). The latter was the superior alternative, owing to its sensitivity and ability to demonstrate small necrotic foci in the temporal lobe (Norris *et al*, 1997). The MRI manifestations of TLN are white-matter lesions (WMLs), cystic components and contrast enhancement in patients with radiation-induced brain injury (Wang *et al*, 2010). Radiologically detected TLN is not always accompanied with neurological symptoms. The TLN patients can present with very subtle symptoms (Lee *et al*, 1988; Van Hasselt and Gibb, 1999).

Most reported cases of radiation-induced TLN were caused by 2D-RT rather than (IMRT). Intensity-modulated radiotherapy is considered an advanced radiation technique for NPC. It differs completely from 2D-RT in terms of plan optimisation, dose delivery and dose escalation, and enables optimal dose distribution in the tumour and organs at risk (Kam *et al*, 2003). According to Marks *et al* (1981), the development of radiation-induced cerebral necrosis was related to the method of radiation delivery, total dose, fraction size, treatment volume and so on. Yet, the differences between 2D-RT-induced and IMRT-induced TLN have not been determined. Here, we evaluated the morphological and clinical features of IMRT-induced TLN and determined its differences from 2D-RT-induced TLN.

MATERIALS AND METHODS

Patient characteristics. From January 2003 to December 2006, we retrospectively recruited consecutive patients with newly diagnosed, non-metastatic and histologically proven NPC curatively treated with RT at Cancer Center, Sun Yat-sen University, Guangzhou, People's Republic of China. The MRI revealed 38 TLN cases among 506 2D-RT-treated patients and 81 TLN cases among 747 IMRT-treated patients. Of the 119 TLN patients whose records were reviewed, 11 were excluded owing to insufficient clinical information or loss to follow-up. The ethics committee of Cancer Center, Sun Yat-sen University, approved this study. Informed consent was obtained from each patient.

The male/female ratio was 3:1 (81 men and 27 women); the median age was 43 years (range, 25–70 years). Histological examination revealed that 99.1% of patients had World Health Organisation (WHO) type 2 disease; 0.9% had WHO type 1 disease. All patients were restaged according to the 2009 7th UICC/AJCC staging system (Edge *et al*, 2010). The overall distribution of patients with stages I, II, III and IVA–B NPC was 11.4%, 22.8%, 30.5% and 35.2%, respectively. No significant between-group difference were found in host factors, histological categories or tumour factors, except for chemotherapy (86.1% (IMRT) *vs* 59.7% (2D-RT), *P* = 0.005; Table 1).

Treatment. All patients received a planned total dose of 68–76 Gy in 2–2.27 Gy fractions at 5 fractions/week using 2D-RT (72 out of 108, 66.7%) or IMRT (36 out of 108, 33.3%). Combination

chemoradiotherapy was used when indicated. Details of the radiotherapy techniques and rationale of using chemotherapy have been published previously (Lai *et al*, 2011; Li *et al*, 2012). In all, 74 out of 108 (68.5%) patients received chemotherapy, and 34 out of 108 (31.1%) patients received radiotherapy alone. Of the 88 patients with stage III/IV disease, 68 (77.3%) received chemotherapy, including various regimens of concurrent chemotherapy combined with induction or adjuvant chemotherapy (73.5%) in conjunction with a platinum-based therapeutic clinical trial. Reasons for deviation from guidelines included age or organ dysfunction that suggested intolerance to chemotherapy.

MRI technique. Magnetic resonance imaging was performed using a 1.5-Tesla system (Signa CV/i, General Electric Healthcare, Chalfont St Giles, UK). If TLN was detected on MRI of the nasopharynx, brain MRI was performed with a head coil. The area from the parietal bone to the lower cerebellar edge was examined. The T1-weighted, fast spin-echo images in the axial, coronal and sagittal planes (repetition time, 500–600 ms; echo time, 10–20 ms; field of view, 25.6 × 25.6 cm; matrix, 512 × 512) and T2-weighted,

Table 1. Patient characteristics			
Characteristic	**2D-RT group** (*n* = 72, %)	**IMRT group** (*n* = 36, %)	**P-value**
Age, years			1.00[a]
<50	54 (75.0%)	27 (75.0%)	
⩾50	18 (25.0%)	9 (25.0%)	
Gender			1.000[a]
Male	54 (75.0%)	27 (76.1%)	
Female	18 (25.0%)	9 (23.6%)	
Pathologic features			0.833[b]
WHO type 1	1 (1.4%)	0 (0.0%)	
WHO type 2	71 (98.6%)	36 (100.0%)	
T category[c]			0.059[a]
T1–2	22 (30.6%)	5 (13.9%)	
T3–4	50 (69.4%)	31 (86.1%)	
N category[c]			0.237[a]
N0–1	55 (76.4%)	31 (86.1%)	
N2–3	17 (23.6%)	5 (13.9%)	
Stage group[c]			0.381[a]
I–II	15 (20.8%)	5 (13.9%)	
III–IV	57 (79.2%)	31 (86.1%)	
Chemotherapy			0.005[a]
CRT	43 (59.7%)	31 (86.1%)	
RT alone	29 (40.3%)	5 (13.9%)	
Hypertension			0.420[b]
Yes	6 (8.3%)	1 (2.8%)	
No	66 (91.7%)	35 (97.2%)	
Diabetes			0.109[b]
Yes	0 (0.0%)	2 (5.6%)	
No	72 (100.0%)	34 (94.4%)	
Smoking			0.722[a]
Yes	29 (59.2%)	16 (44.4%)	
No	42 (40.8%)	20 (55.6%)	

Abbreviations: 2D-RT = two-dimensional radiotherapy; CRT = chemoradiotherapy; IMRT = intensity-modulated radiotherapy; RT = radiotherapy; WHO = World Health Organisation.
[a] *P*-value calculated by the χ^2-test.
[b] *P*-value calculated by Fisher's exact test.
[c] According to the American Joint Committee on Cancer, 7th edition.

fast spin-echo images in the axial plane (repetition time, 4000–6000 ms; echo time, 95–110 ms; field of view, 25.6 × 25.6 cm; matrix, 512 × 512) were obtained before contrast injection. In the axial plane, the section thickness was 5 mm, with a 1-mm interslice gap; in the other planes, the section thickness was 6 mm, with a 1-mm interslice gap. After intravenous injection of gadopentetate dimeglumine (0.1 mmol kg^{-1} body weight; Magnevist, Schering, Berlin, Germany), T1-weighted, spin-echo axial and sagittal sequences and T1-weighted, spin-echo, fat-suppressed coronal sequences were performed sequentially.

MRI analysis. Two radiologists and a clinician specialising in head and neck cancers independently reviewed the MR images. Any disagreements were resolved by consensus. The first MRI showing TLN was reviewed representing the temporal lobe of this side. A diagnosis of MRI-detected TLN required the following criteria:

(a) WMLs: finger-like, hyperintense lesions on T2-weighted images. The size (maximal cross-sectional diameter of largest lesion), location (graded according to distance between outer lesional edge and nasopharynx) and characteristics of signal-intensity abnormalities identified on T2-weighted sequences were reviewed. The WMLs in the temporal lobe were divided into three groups: mild (small focal areas), moderate (larger confluent areas) and severe (large confluent areas extending outside the radiation field with or without local mass effect) (Lee *et al*, 1988).

(b) Contrast-enhanced lesions: lesions with or without necrosis on post-contrast, T1-weighted images with heterogeneous signal abnormalities. Images were reviewed for number, size, extent and characteristics of T1-contrast enhancement. The extent was evaluated using the distance between the outer edge of the CE lesion and the lateral wall of the cavernous sinus (Figure 1). The interior region of enhancement was defined as 'Swiss cheese/soap bubble' when the predominant pattern was multiple, small or medium areas of enhancement intermixed with necrotic foci rather than an area of solid enhancement. The enhancement margin was defined as a 'spreading wave front'' when it was predominantly ill-defined and feathery, and not well demarcated and nodular (Rogers *et al*, 2011).

(c) Cysts: round or oval, well-defined, highly hyperintense lesions on T2-weighted images, with a thin or imperceptible wall. Cysts were evaluated for size and number.

(d) Local mass effect: shifting of the brain structures owing to the TLN nidus. Local mass effect was classified as mild (affecting only the temporal lobe sulci), moderate (affecting the sulci and ventricles) and severe (affecting the midline of the brain; Figure 2).

Follow-up and statistical analysis. Patients were followed up at least every 3 months during the first 2 years, and then every 6 months until death. Their symptoms and signs were recorded by physicians in an outpatient clinic. Patients who failed to return to the clinic were contacted by telephone. Follow-up MRI of the nasopharynx and/or neck was performed every 6–12 months or when emerging symptoms/signs suggested recurrence or neurologic dysfunction.

The Statistical Package for Social Sciences, version 13.0 (SPSS, Chicago, IL, USA) was used for all statistical analyses. The independent-samples t-test was used to calculate between-group differences in continuous variables. Other characteristics were compared using the χ^2-test or Fisher's exact test. Univariate analysis was used to detect significant factors. Multivariate analysis using the Cox proportional hazards model was used to test independent significance by backward elimination of insignificant explanatory variables. Imaging features were included as covariates

in all tests. Statistical significance was set at $\alpha = 0.05$; P-values were based on two-sided tests.

RESULTS

Temporal lobe necrosis was unilateral in 38 patients and bilateral in 70 patients. Bilateral TLN was significantly more common in the 2D-RT group (56 out of 72, 77.8%) than in the IMRT group (14 out of 36, 27.8%, $P < 0.001$). There were 128 and 50 injured temporal lobes in the 2D-RT and IMRT groups, respectively. The median interval between radiotherapy and MRI confirmation of TLN was 44.5 months (range, 14.4–87.6 months). The median latency of symptomatic TLN was 50.1 months (range, 16.2–58.3 months).

MRI appearance

WMLs. White-matter lesions were present in 128 out of 128 (100.00%) and 48 out of 50 (94.44%) temporal lobes in the 2D-RT and IMRT groups, respectively ($P = 0.078$). Their mean maximum diameter was 40.9 mm (range, 3.0–100.4 mm) in the 2D-RT group and 37.3 mm (range, 8.9–88.9 mm) in the IMRT group ($P = 0.326$, Figure 2). The WMLs were mild in 53 out of 128 (41.4%), moderate in 34 out of 128 (26.6%) and severe in 41 out of 128 (32.0%) temporal lobes in the 2D-RT group. The corresponding values in the IMRT group were 36 out of 48 (75.0%), 9 out of 48 (18.8%) and 3 out of 48 temporal lobes (6.3%, $P < 0.001$; Table 2).

Contrast-enhanced lesions. Contrast-enhanced lesions were present on T1-weighted images in 123 out of 128 (96.1%) and 47 out of 50 (94.0%) temporal lobes in the 2D-RT and IMRT groups, respectively ($P = 0.688$; Table 2). Their mean maximum diameter was 22.4 mm (range, 5.2–92.0 mm) and 15.6 mm (range, 3.4–43.5 mm) in the 2D-RT and IMRT groups, respectively ($P < 0.001$, Figure 1). The lesion features were similar in both groups, except that spreading wavefronts were more likely in the 2D-RT group, and nodular enhancement was more common in the IMRT group ($P = 0.001$). These lesions were more likely to extend far away from the nasopharynx in both the mediolateral and superoinferior directions in the 2D-RT group ($P < 0.001$ and $P = 0.009$, respectively).

Cysts. Cysts were present in 10 out of 128 (7.8%) and 1 out of 50 (2%) temporal lobes in the 2D-RT and IMRT groups, respectively ($P = 0.185$). Their maximum diameter was 5.8–67.3 mm (mean, 30.93 mm) in the 2D-RT group. Most patients had a single cyst, except for one patient in the 2D-RT group who had multiple cysts in a lobe and two patients in the 2D-RT group who had bilateral cysts (Figure 3). Neither WMLs nor contrast-enhanced lesions had any impact on cyst development (both $P = 1$).

Local mass effect. We observed local mass effects in 57 out of 128 (44.5%) and 13 out of 50 (26.0%) temporal lobes in the 2D-RT and IMRT groups, respectively ($P = 0.023$). The between-group difference in the severity of these effects was of marginal significance ($P = 0.095$). Local mass effects were always associated with contrast-enhanced lesions ($P = 0.024$) but were not correlated with WMLs or cysts ($P = 0.523$ and 0.341, respectively).

Clinical features. Of the 108 patients, 46 (42.6%) presented with mild symptoms (mild memory impairment, personality change and/or occasional dizziness), and 27 (25.0%) had nonspecific features of intracranial lesions such as mild headache, mental confusion and/or generalised convulsions. Fifteen patients (13.9%) were seriously affected with marked debilitation, pressure symptoms, epileptic attacks and/or changes in consciousness level. The remaining 20 patients (18.5%) had no symptoms or signs indicative of TLN. The most frequent symptoms and/or signs
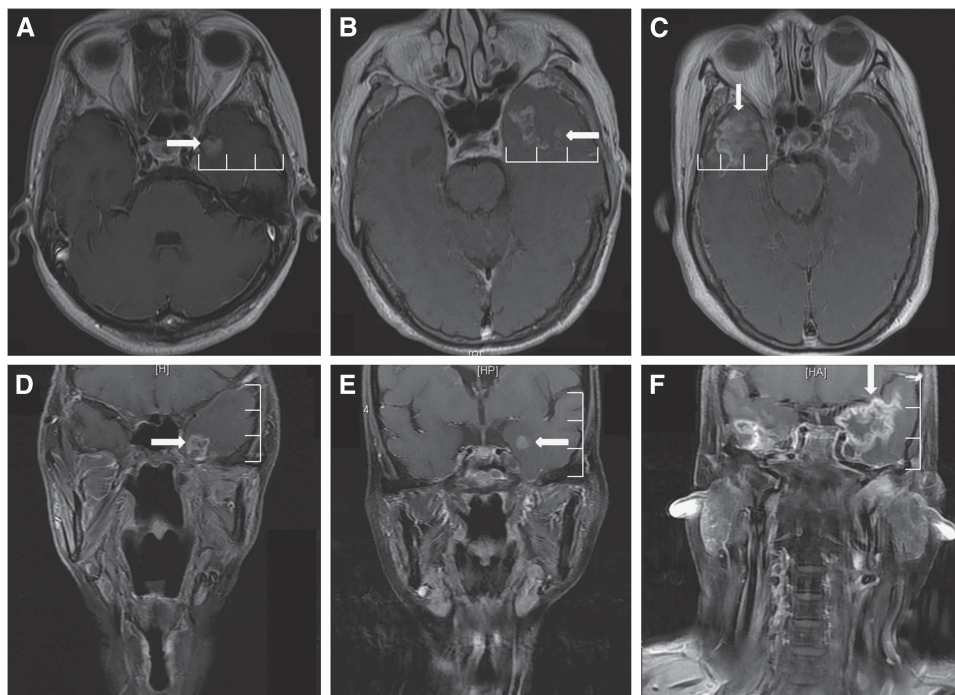
Figure 1. Post-contrast, T1-weighted magnetic resonance images show the extent of contrast-enhanced lesions in both the mediolateral and superoinferior directions. (A) Contrast-enhanced lesions (rightward arrow) within the medial 1/3 of the ipsilateral temporal lobe in an axial image. (B) Contrast-enhanced lesions (leftward arrow) extending beyond the medial 1/3 but not reaching the lateral 1/3 of the ipsilateral temporal lobe in an axial image. (C) Contrast-enhanced lesions (downward arrow) reaching the lateral 1/3 of the ipsilateral temporal lobe in an axial image. (D) Contrast-enhanced lesions (rightward arrow) within the inferior 1/3 of the ipsilateral temporal lobe in a coronal image. (E) Contrast-enhanced lesions (leftward arrow) extending beyond the inferior 1/3 but not reaching the superior 1/3 of the ipsilateral temporal lobe in a coronal image. (F) Contrast-enhanced lesions (downward arrow) reaching the superior 1/3 of the ipsilateral temporal lobe in a coronal image.
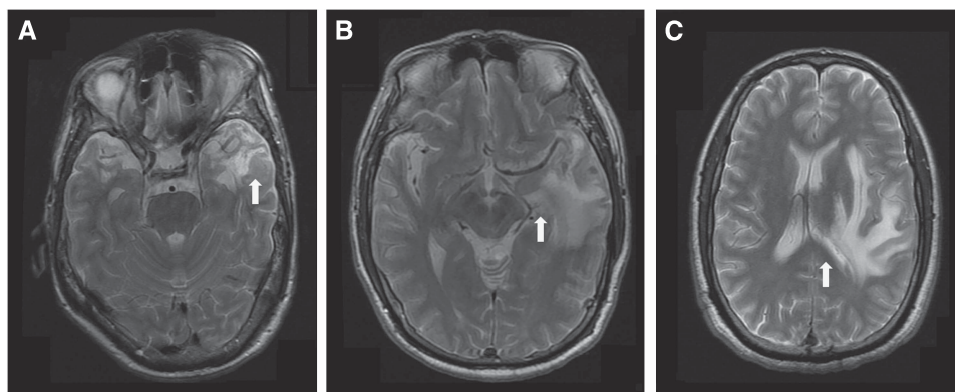

Figure 2. Axial T2-weighted magnetic resonance images showing the severity of local mass effects. (A) Mild local mass effect affecting only the sulci of the temporal lobe (white arrow). (B) Moderate local mass effect affecting the sulci and ventricle (white arrow). (C) Severe local mass effect affecting the midline (white arrow).

were headache (46.3%), hearing disorder (44.4%) and dizziness (37.0%). There were no obvious between-group differences in clinical features (all P-values > 0.05; Table 3). The median latency of symptomatic TLN was shorter in the 2D-RT group than in the IMRT group (42.85 vs 56.77 months, $P = 0.005$).

The between-group difference in the incidence of severe debility was of marginal significance (18.1% vs 5.6%, $P = 0.077$). On univariate analysis, five factors (extent of WMLs, size of contrast-enhanced lesions, locations of contrast-enhanced lesions in the mediolateral and superoinferior directions, cysts and local mass effects) were significantly correlated with deteriorating symptoms ($P < 0.001$, $P = 0.005$, $P < 0.001$, $P < 0.001$, $P < 0.001$ and $P = 0.01$, respectively). Multivariate analysis was performed to test independent significance; the following parameters were included as

covariates: WMLs (yes vs no), size of WMLs (< 40 vs > 40 mm), severity of WMLs, extent of contrast-enhanced lesions (yes vs no), size of contrast-enhanced lesions (< 34 vs > 34 mm), peripheral enhancement pattern, interior enhancement pattern, locations of enhancement in the mediolateral and superoinferior directions, cysts (yes vs no), cyst size (< 30 vs > 30 mm) and local mass effect (yes vs no). Forward inclusion of significant explanatory variables showed that the extent of enhancement in the mediolateral direction (hazard ratio (HR) = 2.563, 95% confidence interval (CI) for HR = (1.732–4.021), $P < 0.001$) and cysts (HR = 0.481, 95% CI for HR = (0.289–0.665), $P < 0.001$) independently predicted devastating symptoms. It seemed patients with enhancing lesion(s) extending to the lateral border of the temporal lobe and/or those with cyst(s) were more likely to suffer devastating symptoms.

Table 2. MRI characteristics of temporal lobe necrosis			
Characteristic	**2D-RT group**	**IMRT group**	**_P_-value**
WMLs			
Temporal lobes (number)	128 out of 128 (100%)	48 out of 50 (94.44%)	0.078[a]
Size (mm)	40.9	37.3	0.326[b]
Severity of WMLs			< 0.001[a]
Mild	53 out of 128 (41.4%)	36 out of 48 (75.0%)	
Moderate	34 out of 12863 (26.6%)	9 out of 48 (18.8%)	
Severe	41 out of 128 (32.0%)	3 out of 48 (6.3%)	
Contrast-enhanced lesions			
Temporal lobes (number)	123 out of 128 (96.1%)	47 out of 50 (94.0%)	0.688[a]
Size (mm)	22.4	15.6	< 0.001[b]
Pattern of peripheral enhancement			0.001[c]
Spreading wavefront	102 out of 123 (82.9%)	28 out of 47 (59.6%)	
Nodular	21 out of 123 (17.1%)	19 out of 47 (40.4%)	
Pattern of interior enhancement			0.091[c]
Swiss cheese/soap bubble	85 out of 123 (69.1%)	26 out of 47 (55.3%)	
Solid	38 out of 123 (30.9%)	21 out of 47 (44.7%)	
Number of enhancing lesions			0.129[c]
Single lesion	68 out of 123 (55.3%)	32 out of 47 (68.1%)	
Multiple lesions	55 out of 123 (44.7%)	15 out of 47 (31.9%)	
Location in the mediolateral direction			< 0.001[c]
Located within the medial 1/3	15 out of 123 (12.2%)	21 out of 47 (44.7%)	
Between the medial 1/3 and lateral 1/3	33 out of 123 (26.8%)	18 out of 47 (38.3%)	
Spread to the lateral 1/3	75 out of 123 (61.0%)	8 out of 47 (17.0%)	
Location in the superoinferior direction			0.009[a]
Located within the inferior 1/3	11 out of 123 (8.9%)	8 out of 47 (17.0%)	
Between the inferior 1/3 and superior 1/3	88 out of 123 (71.6%)	38 out of 47 (80.9%)	
Spread to the superior 1/3	24 out of 123 (19.5%)	1 out of 47 (2.1%)	
Cysts			
Temporal lobes (number)	10 out of 128 (7.8%)	1 out of 50 (2%)	0.185[a]
Size (mm)	30.9	19.8	0.619[b]
Local mass effect			0.095[a]
None	71 out of 128 (55.5%)	37 out of 50 (74.0%)	
Sulci	24 out of 128 (18.8%)	6 out of 50 (12.0%)	
Sulci and ventricle	25 out of 128 (19.5%)	4 out of 50 (8.0%)	
Sulci, ventricle and midline	8 out of 128 (6.3%)	3 out of 50 (6.2%)	

Abbreviations: 2D-RT = two-dimensional radiotherapy; IMRT = intensity-modulated radiotherapy; MRI = magnetic resonance imaging; WML = white-matter lesion.
[a]_P_-values calculated by Fisher's exact test.
[b]_P_-values calculated by the independent-samples _t_-test.
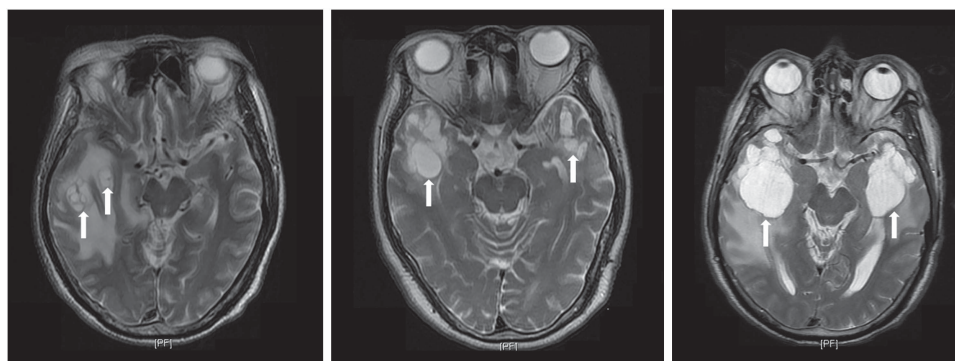[c]_P_-values calculated by the χ^2-test.

Figure 3. Representative axial T2-weighted magnetic resonance images in patients with multiple cysts in the temporal lobe.

Table 3. Presenting symptoms and signs in patients with TLN induced by 2D-RT or IMRT			
Clinical feature	2D-RT group (n = 72, %)	IMRT group (n = 36, %)	P-value
Symptom			
Dizziness	26 (36.1%)	14 (38.9%)	0.778[a]
Memory impairment	24 (33.3%)	12 (33.3%)	1.000[a]
Personality changes	18 (29.0%)	12 (33.3%)	0.656[a]
Temporal lobe epilepsy	20 (27.8%)	13 (36.1%)	0.375[a]
Headache	35 (45.5%)	15 (41.7%)	0.706[a]
Mental confusion	11 (15.3%)	5 (13.9%)	0.848[a]
Generalised convulsion	6 (8.3%)	2 (5.6%)	0.716[b]
Diplopia	2 (2.8%)	0 (0.0%)	0.551[b]
Hallucination	8 (11.1%)	3 (8.3%)	0.748[b]
Dysphasia (including motor or sensory aphasia)	3 (4.2%)	1 (2.8%)	1.000[b]
Hearing disorder	30 (41.7%)	18 (35.3%)	0.475[a]
Ataxia	6 (8.3%)	2 (5.6%)	0.716[b]
Visual field defect	4 (5.6%)	1 (2.8%)	0.663[b]
Nystagmus	8 (11.1%)	3 (8.3%)	0.748[b]
None	9 (12.5%)	8 (22.2%)	0.191[a]
Signs			
Coma	10 (13.9%)	4 (11.1%)	0.770[b]
Sixth cranial nerve palsy	9 (12.5%)	3 (8.3%)	0.747[b]
Facial paralysis	6 (8.3%)	2 (5.6%)	0.716[b]
Upper limbs paralysis	13 (18.1%)	5 (13.9%)	0.584[a]
Papilloedema	5 (6.9%)	2 (5.6%)	1.000[b]
Global dysphasia	1 (1.4%)	0 (0.0%)	1.000[b]
None referable to temporal lobe	58 (80.6%)	30 (83.3%)	0.726[a]

Abbreviations: 2D-RT = two-dimensional radiotherapy; IMRT = intensity-modulated radio-therapy; TLN = temporal lobe necrosis.
[a]P-values calculated by the χ^2-test.
[b]P-values calculated by Fisher's exact test.

DISCUSSION

Intensity-modulated radiotherapy is a common treatment modality and is ideal for NPC. However, the differences between the imaging and clinical characteristics of IMRT-induced TLN *vs* 2D-RT-induced TLN remain poorly understood. A comprehensive understanding of the features of IMRT-induced TLN may facilitate its accurate diagnosis and appropriate management.

Evolution of radiation-induced TLN. Wang *et al* (2010) assessed the evolution of radiation-induced injury, and found that WMLs developed first followed by contrast-enhanced lesions; cysts were the least frequent manifestation and occurred in the late stages of TLN. Our observations are consistent with these findings. The WMLs occurred in almost all injured lobes (98.9%); their predominance could be attributed to the predominance of the pathological changes of TLN in the white matter. Mahaley *et al* (1977) identified the predominant pathology of radiation-induced brain injury as white-matter demyelination, coagulative necrosis, vacuolar change and oedema.

Contrast-enhanced lesions always occurred in the presence of WMLs. In our study, contrast enhancement appeared in 95.5% of the affected lobes. Rogers *et al* (2011) suspected that enhancement was because of prominent vascular changes associated with radiation-induced injury. Experimental models have also suggested that brain microvasculature damage is the primary event in the development of late radiation-induced brain injury

(Coderre *et al*, 2006). However, histological confirmation was not obtained in our study.

Cysts were the least frequent pattern of radiation-induced injury, occurring in <10% of cases. This prevalence is lower than the previously reported rates of 12.7–15.7% (Lee *et al*, 1988; Wang *et al*, 2010). This inconsistency may be attributable to the inclusion of brain tumours other than NPC; the pre-existing brain tumour or surgical alterations may have obscured the imaging findings of radiation-induced cysts in the previous studies. Wang *et al* (2010) reported that cysts were always accompanied by both WMLs and contrast-enhanced lesions. However, we found that cysts were not correlated with either of these. One possible explanation for this difference is that our study may have contained too few cases of cysts to reach statistical significance.

Imaging features of TLN induced by 2D-RT or IMRT. For decades, NPC was treated with conventional 2D-RT that mainly consists of opposed lateral fields focussed on the primary tumour to deliver tumouricidal doses. Unlike 2D-RT, IMRT involves multiple small beam segments (pencil beams), with neighbouring beams having varying intensities. Beams with different intensities collectively produce dose distributions conforming to the required target shape (Kam *et al*, 2003). The features of radiation-induced TLN varied with radiation patterns as follows.

First, significantly more patients in the 2D-RT group developed bilateral TLN. As the inferior portions of the temporal lobes lie within the radiation portals of 2D-RT, TLN often occurred in the inferomedial parts of both temporal lobes. Second, 2D-RT-induced TLN lesions were more extensive, being both wider in range and larger in size, and showing greater contrast enhancement. In 2D radiotherapy, shielding was based on bony landmarks without volumetric contouring of the structures. As a result, the radiation volume and doses delivered to the temporal lobe might have been underestimated. Kumar *et al* (2000) determined that enhancing radiation-induced necrosis occurred within the treatment volume. Thus, this phenomenon may reflect the large volume and high dose to the temporal lobe in 2D-RT compared with IMRT. Lastly, the most common enhancement pattern in the 2D-RT group was the 'spreading wave front' that was uncommon in the IMRT group. This enhancement pattern may represent a more severe, later stage of TLN (Rogers *et al*, 2011). However, we did not assess the histopathology of these enhancement patterns.

Clinical manifestations of TLN. No obvious differences in clinical manifestations were detected between the two groups. One possible reason for this is that the MRI abnormalities appeared before clinical symptoms; most cases were incidentally detected while the patient was being followed up for other clinical indications. Up to 61% of the patients had vague or no symptoms; these cases may be missed if physicians do not have a high index of suspicion (Norris *et al*, 1997). In addition, the subjective complaints of the patients may have correlated poorly with objective radiologic evidence because of the complexity of the brain (Hsiao *et al*, 2010). The temporal lobes are responsible for memory and language. A major manifestation of TLN was memory impairment (Bonelli *et al*, 2010), usually because of an obscure cause. Besides radiation, many interacting factors may affect memory in NPC patients, including the underlying neuropathology, seizure activity, anticonvulsants, surgery, age, genetics and psychosocial factors (Butler and Zeman, 2008).

Our data demonstrated that patients with enhancing lesion(s) extending to the lateral border of the temporal lobe were vulnerable to devastating symptoms. Unlike the small nidus that may be compensated for by the adjacent normal brain tissue, larger lesions of the temporal lobe were unlikely to regress and could become symptomatic and impair function. Cysts were another independent predictor of devastating symptoms, probably because

cysts developed in the later phase of necrosis and were associated with higher radiation doses.

Limitations. As this was a retrospective study, regular follow-up MRI for all patients was scarcely possible. As TLN is an evolving, dynamic process whose morphological, imaging and clinical characteristics may change over time, irregular MRI may have confounded the study results to a certain extent. We did not use cognition-specific scales/examinations to evaluate temporal lobe-related functions. Lastly, because of the absence of serious clinical symptoms that would justify exploratory surgery and because temporal lobectomy would be hazardous in patients with bilateral involvement, TLN typically lacked histological verification.

CONCLUSIONS

To our knowledge, this is the first study to focus on the differences in the radiological and clinical features of 2D-RT-induced *vs* IMRT-induced TLN. The radiological manifestations of 2D-RT-induced TLN were more extensive and severe than those of IMRT-induced TLN, but the clinical features were similar. Our findings could facilitate the timely diagnosis and appropriate management of TLN after radiotherapy for NPC.

ACKNOWLEDGEMENTS

CONFLICT OF INTEREST

The authors declare no conflict of interest.

REFERENCES

Bonelli SB, Powell RH, Yogarajah M, Samson RS, Symms MR, Thompson PJ, Koepp MJ, Duncan JS (2010) Imaging memory in temporal lobe epilepsy: predicting the effects of temporal lobe resection. *Brain* **133**(Pt 4): 1186–1199.

Butler CR, Zeman AZ (2008) Recent insights into the impairment of memory in epilepsy: transient epileptic amnesia, accelerated long-term forgetting and remote memory impairment. *Brain* **131**(Pt 9): 2243–2263.

Coderre JA, Morris GM, Micca PL, Hopewell JW, Verhagen I, Kleiboer BJ, van der Kogel AJ (2006) Late effects of radiation on the central nervous system: role of vascular endothelial damage and glial stem cell survival. *Radiat Res* **166**(3): 495–503.

Edge SB, Byrd DR, Compton CC, Fritz AG, Greene FL, Trotti A. American Joint Committee on Cancer (2010) *AJCC Cancer Staging Manual*. 7th edn. Springer: New York.

Hsiao KY, Yeh SA, Chang CC, Tsai PC, Wu JM, Gau JS (2010) Cognitive function before and after intensity-modulated radiation therapy in patients with nasopharyngeal carcinoma: a prospective study. *Int J Radiat Oncol Biol Phys* **77**(3): 722–726.

Jemal A, Bray F, Center MM, Ferlay J, Ward E, Forman D (2011) Global cancer statistics. *CA Cancer J Clin* **61**(2): 69–90.

Kam MK, Chau RM, Suen J, Choi PH, Teo PM (2003) Intensity-modulated radiotherapy in nasopharyngeal carcinoma: dosimetric advantage over conventional plans and feasibility of dose escalation. *Int J Radiat Oncol Biol Phys* **56**(1): 145–157.

Kumar AJ, Leeds NE, Fuller GN, Van Tassel P, Maor MH, Sawaya RE, Levin VA (2000) Malignant gliomas: MR imaging spectrum of radiation therapy- and chemotherapy-induced necrosis of the brain after treatment. *Radiology* **217**(2): 377–384.

Lai SZ, Li WF, Chen L, Luo W, Chen YY, Liu LZ, Sun Y, Lin AH, Liu MZ, Ma J (2011) How does intensity-modulated radiotherapy versus conventional two-dimensional radiotherapy influence the treatment results in nasopharyngeal carcinoma patients? *Int J Radiat Oncol Biol Phys* **80**(3): 661–668.

Lee AW, Cheng LO, Ng SH, Tse VK, O SK, Au GK, Poon YF (1990) Magnetic resonance imaging in the clinical diagnosis of late temporal lobe necrosis following radiotherapy for nasopharyngeal carcinoma. *Clin Radiol* **42**(1): 24–31.

Lee AW, Law SC, Ng SH, Chan DK, Poon YF, Foo W, Tung SY, Cheung FK, Ho JH (1992) Retrospective analysis of nasopharyngeal carcinoma treated during 1976-1985: late complications following megavoltage irradiation. *Br J Radiol* **65**(778): 918–928.

Lee AW, Ng SH, Ho JH, Tse VK, Poon YF, Tse CC, Au GK, O SK, Lau WH, Foo WW (1988) Clinical diagnosis of late temporal lobe necrosis following radiation therapy for nasopharyngeal carcinoma. *Cancer* **61**(8): 1535–1542.

Li WF, Sun Y, Chen M, Tang LL, Liu LZ, Mao YP, Chen L, Zhou GQ, Li L, Ma J (2012) Locoregional extension patterns of nasopharyngeal carcinoma and suggestions for clinical target volume delineation. *Chin J Cancer* **31**(12): 579–587.

Mahaley Jr MS, Vogel FS, Burger P, Ghatak NR (1977) Neuropathology of tissues from patients treated by the Brain Tumor Study Group. *Natl Cancer Inst Monogr* **46**: 77–82.

Marks JE, Baglan RJ, Prassad SC, Blank WF (1981) Cerebral radionecrosis: incidence and risk in relation to dose, time, fractionation and volume. *Int J Radiat Oncol Biol Phys* **7**(2): 243–252.

Norris AM, Carrington BM, Slevin NJ (1997) Late radiation change in the CNS: MR imaging following gadolinium enhancement. *Clin Radiol* **52**(5): 356–362.

Rogers LR, Gutierrez J, Scarpace L, Schultz L, Ryu S, Lord B, Movsas B, Honsowetz J, Jain R (2011) Morphologic magnetic resonance imaging features of therapy-induced cerebral necrosis. *J Neurooncol* **101**(1): 25–32.

Van Hasselt A, Gibb AG (1999) *Nasopharyngeal Carcinoma*. 2nd edn. Chinese University Press; Greenwich Medical Media: Hong Kong. London.

Wang YX, King AD, Zhou H, Leung SF, Abrigo J, Chan YL, Hu CW, Yeung DK, Ahuja AT (2010) Evolution of radiation-induced brain injury: MR imaging-based study. *Radiology* **254**(1): 210–218.